

Suppression of the Superconducting Transition in $R\text{FeAsO}_{1-x}\text{F}_x$ for $R = \text{Tb, Dy, Ho}$

Jennifer A. Rodgers,^{1,2} George B. S. Penny,^{1,2} Andrea Marcinkova,^{1,2} Jan-Willem G. Bos,
^{1,2} Dmitry A. Sokolov,^{1,3} Anna Kusmartseva,^{1,2} Andrew D. Huxley^{1,3} and J. Paul
Attfield^{1,2*}

¹*Centre for Science at Extreme Conditions, University of Edinburgh, King's Buildings,
Mayfield Road, Edinburgh, EH9 3JZ.*

²*School of Chemistry, University of Edinburgh, Edinburgh, EH9 3JJ.*

³*SUPA, School of Physics, University of Edinburgh, Edinburgh, EH9 3JZ.*

A suppression of superconductivity in the late rare earth $R\text{FeAsO}_{1-x}\text{F}_x$ materials is reported. The maximum critical temperature (T_c) decreases from 51 K for $R = \text{Tb}$ to 36 K for $\text{HoFeAsO}_{0.9}\text{F}_{0.1}$, which has been synthesised under 10 GPa pressure. This suppression is driven by a decrease in the Fe-As-Fe angle below an optimum value of 110.6° , as the angle decreases linearly with unit cell volume (V) across the $R\text{FeAsO}_{1-x}\text{F}_x$ series. A crossover in electronic structure around this optimum geometry is evidenced by a change in sign of the compositional dT_c/dV , from negative values for previously reported large R materials to positive for $\text{HoFeAsO}_{0.9}\text{F}_{0.1}$.

Rare earth (R) oxypnictides $R\text{FeAsO}$ ¹ were recently discovered to superconduct when doped, with critical temperatures surpassed only by the high- T_c cuprates. Several families of superconducting iron pnictides have subsequently been

discovered.² These all have layered structures containing AsFeAs slabs with Fe tetrahedrally coordinated by As. The main types are the 1111 materials based on $R\text{FeAsO}$ or $M\text{FeAsF}$ ($M = \text{Ca, Sr, Ba}$), the 122 phases $M\text{Fe}_2\text{As}_2$, and the 111 $A\text{FeAs}$ ($A = \text{Li, Na}$) family. The related binaries FeX ($X = \text{Se, Te}$) are also superconducting.

The electron-doped 1111 materials $R\text{FeAsO}_{1-x}\text{F}_x$ and $R\text{FeAsO}_{1-\delta}$ materials remain prominent as they have the highest T_c 's, up to 56 K, and allow lattice and doping effects to be investigated through variations of the R^{3+} cation size and the anion composition. A strong lattice effect is evident at the start of the rare earth series, as T_c rises from 26 K for $\text{LaFeAsO}_{1-x}\text{F}_x$ to 43 K under pressure,^{3,4} and to a near-constant maximum 50-56 K in the $R\text{FeAsO}_{1-x}\text{F}_x$ and $R\text{FeAsO}_{1-\delta}$ series for $R = \text{Pr}$ to Gd ,^{5,6,7,8,9,10} but whether lattice effects ultimately enhance or suppress superconductivity for the late R 's has been unclear. The late rare earth $R\text{FeAsO}_{1-x}\text{F}_x$ materials and the oxygen-deficient $R\text{FeAsO}_{1-\delta}$ superconductors require high pressure synthesis, leading to significant challenges as single phase samples are difficult to prepare, and accurate analyses of cation stoichiometries and O and F contents are difficult. To investigate the effect of the lattice for later R we have synthesised multiple samples of $R\text{FeAsO}_{0.9}\text{F}_{0.1}$ ($R = \text{Tb, Dy, and Ho}$) under varying high pressure conditions. Here we report superconductivity in $\text{HoFeAsO}_{0.9}\text{F}_{0.1}$ for which the maximum T_c of 36 K is markedly lower than in the previous R analogs. This is part of a systematic suppression of superconductivity by the smaller, late R cations. $\text{HoFeAsO}_{0.9}\text{F}_{0.1}$ also shows a reversal in the sign of the compositional dT_c/dV ($V = \text{unit cell volume}$) compared to the early R materials, confirming that the decreasing R size has a significant effect on the bands contributing to the Fermi surface.

Polycrystalline ceramic $R\text{FeAsO}_{1-x}\text{F}_x$ samples ($R = \text{Tb, Dy, and Ho}$) were synthesised by a high pressure method and investigated by powder X-ray diffraction, magnetization and conductivity measurements.¹¹ Initial results for $R\text{FeAsO}_{1-x}\text{F}_x$ ($R = \text{Tb and Dy}$) were published elsewhere.¹² Both materials were found to be superconducting with maximum T_c 's of 46 and 45 K respectively. Little difference in superconducting properties between samples with nominal compositions of $x = 0.1$ and 0.2 were observed, and the $x = 0.2$ materials were generally of lower phase purity, and so the $x = 0.1$ composition was used in subsequent syntheses. The best samples typically contain ~80% by mass of the superconducting phase with residual non-superconducting $R_2\text{O}_3$ and $R\text{As}$ phases also present. The sample purity and superconducting properties are not sensitive to synthesis pressure over a range that moves to higher pressures as R decreases in size; $R = \text{Tb and Dy}$ superconductors were respectively prepared at 7-10 and 8-12 GPa, heating at 1050-1100 °C. Repeated syntheses of $\text{TbFeAsO}_{1-x}\text{F}_x$ gave several samples with higher T_c 's than the above value, the highest value is $T_c(\text{max}) = 51 \text{ K}$ (Fig. 1). Further $\text{DyFeAsO}_{1-x}\text{F}_x$ samples did not show higher transitions than before, so we conclude that $T_c(\text{max})$ in this system is 45 K.

Tetragonal $\text{HoFeAsO}_{0.9}\text{F}_{0.1}$ was obtained from reactions at 10 GPa pressure and the properties of six $\text{HoFeAsO}_{0.9}\text{F}_{0.1}$ samples prepared under varying conditions are summarized in Table 1. Crystal structure refinements and phase analysis were carried out by fitting powder X-ray diffraction data (Fig. 2).¹³ Magnetisation measurements demonstrate that all six $\text{HoFeAsO}_{1-x}\text{F}_x$ samples are bulk superconductors with T_c 's of 29-36 K (Fig. 3). Resistivities show smooth high temperature evolutions without apparent

spin density wave anomalies. The transitions to the zero resistance state have widths of less than 4 K.

Although all of the samples in Table 1 have the same starting composition, small variations of synthesis pressure and temperature result in a dispersion in x around the nominal 0.1 value for the $\text{HoFeAsO}_{1-x}\text{F}_x$ phase and corresponding variations in superconducting properties. T_c increases to a maximum value, $T_c(\text{max})$, at the upper solubility limit of x in $R\text{FeAsO}_{1-x}\text{F}_x$ systems,⁷ and this is consistent with the observation that the superconducting phases in samples 1, 3 and 4, which are heated at high temperatures or longer times and so are likely to have a slightly lower F content, have lower T_c 's (average 32.1 K) than the other three samples, made under nominally identical 'optimum' conditions, which have average $T_c = 34.8$ K. Sample 6 shows the highest $T_c = 36.2$ K and the lowest proportion of the $\text{HoFeAsO}_{1-x}\text{F}_x$ phase and a correspondingly low diamagnetic volume fraction. This demonstrates that the sample is at the upper limit of the superconducting composition range and so gives a realistic $T_c(\text{max})$ for the $\text{HoFeAsO}_{1-x}\text{F}_x$ system.

Although the doping values x for the high pressure $R\text{FeAsO}_{1-x}\text{F}_x$ samples are not known precisely, comparing ensembles of samples with similar phase purities made under similar conditions reveals a clear suppression of superconductivity by lattice effects for heavier R . For example, all of our $\text{TbFeAsO}_{1-x}\text{F}_x$ superconductors have higher T_c 's (five $\text{TbFeAsO}_{1-x}\text{F}_x$ samples, $T_c = 45\text{-}51$ K) than all of the $\text{HoFeAsO}_{1-x}\text{F}_x$ materials (in Table 1). The $T_c(\text{max})$ values of 51, 45 and 36 K for $R\text{FeAsO}_{1-x}\text{F}_x$ with $R = \text{Tb}, \text{Dy}$ and Ho , respectively thus represent the trend correctly.

Fig. 4 shows a plot of the maximum critical temperatures, $T_c(\text{max})$, against unit cell volume for many reported $R\text{FeAsO}_{1-x}\text{F}_x$ and $R\text{FeAsO}_{1-\delta}$ systems and our above materials. $T_c(\text{max})$ rises slowly as cell volume decreases for $R = \text{La}$ to Pr and then shows a broad maximum, between $R = \text{Pr}$ and Tb in the $R\text{FeAsO}_{1-x}\text{F}_x$ materials, before falling rapidly as R changes from Tb to Dy to Ho . This trend is not seen in the reported $R\text{FeAsO}_{1-x}$ superconductors, where $T_c(\text{max})$ remains approximately constant,^{14,15} apparently because they have larger cell volumes than their $R\text{FeAsO}_{1-x}\text{F}_x$ analogs (see Fig. 4).

The size of the R^{3+} cation tunes the electronic properties through variations in the geometry of the FeAs slab. A trend between the As-Fe-As (or equivalent Fe-As-Fe) angle and T_c has been reported for the early R materials.¹⁶ The upper panel of Fig. 4 shows representative reported values for optimal $R\text{FeAsO}_{1-x}\text{F}_x$ superconductors including our $R = \text{Tb}$, Dy , and Ho materials. This demonstrates that the angle decreases monotonically with R size and so does not show a universal correlation with $T_c(\text{max})$. The $T_c(\text{max})$ variation in the $R\text{FeAsO}_{1-x}\text{F}_x$ series is described by a simple $\cos(\phi - \phi_0)$ function, shown in Fig. 4, where the value of the As-Fe-As angle corresponding to the global maximum T_c , $\phi_{\text{max}} = 110.6^\circ$, is close to the ideal 109.5° value for a regular FeAs_4 tetrahedron. All five of the Fe 3d-bands are partially occupied and contribute to the Fermi surface of the iron arsenide superconductors through hybridization with As 4s and 4p states.¹⁷ Decreasing the tetrahedral angle through 109.5° marks the crossover from tetragonal compression to elongation of the FeAs_4 tetrahedra. In a crystal field model, this reverses the splittings of the t_2 and e d-orbital sets and so a significant crossover in the real electronic structure is likely to occur near 109.5° .

Evidence for the above crossover also comes from a discovered change in the sign of the compositional dT_c/dV near optimum doping in the $RFeAsO_{1-x}F_x$ systems.¹⁸ The unit cell parameters and volume for the six $HoFeAsO_{1-x}F_x$ samples in Table 1 show a positive correlation with T_c (Fig. 5), in contrast to early $R = La$ ¹⁹ and Sm ⁷ analogs where lattice parameters and volume decrease with increasing T_c . The T_c, V points for near-optimally doped $R = La, Sm$ and Ho $RFeAsO_{1-x}F_x$ superconductors are shown on Fig. 4 together with the derived dT_c/dV values. dT_c/dV for a single $RFeAsO_{1-x}F_x$ system follows the overall trend in $dT_c(max)/dV$ for different R 's, changing from a negative value at large $R = La$ to a small positive slope at $R = Ho$.

The compositional dT_c/dV for a given $RFeAsO_{1-x}F_x$ system reflects two competing effects of variations in the fluoride content x on the lattice volume. F^- is slightly smaller than O^{2-} so the anion substitution effect gives a negative contribution to the compositional dT_c/dV , independent of R . The concomitant effect of doping electrons into the Fe d-bands tends to expand the lattice (and increase T_c), but the magnitude of this positive dT_c/dV term depends on the nature of the bands at the Fermi surface. The observed shift from negative to positive dT_c/dV as R changes from La to Ho shows that the decreasing size of the R^{3+} cation leads to significant changes in the Fermi surface, with volume-expanding (antibonding) bands more prominent for smaller R . Calculations have confirmed that the electronic structure near the Fermi level is sensitive to such small changes in the As z-coordinate (equivalent to changing the Fe-As-Fe angle).²⁰ Small changes in the contributions of the d-bands are likely to be particularly important in a multigap scenario for superconductivity, as evidenced in gap measurements of $TbFeAsO_{0.9}F_{0.1}$ and other iron arsenide materials.²¹

In summary, our analysis of multiple samples of $R\text{FeAsO}_{1-x}\text{F}_x$ ($R = \text{Tb, Dy, and Ho}$) superconductors demonstrates that the maximum critical temperature falls from 51 K for $R = \text{Tb}$ to 36 K for the previously unreported Ho analog. Hence, the effect on the lattice of substituting smaller, late rare earths in the $R\text{FeAsO}_{1-x}\text{F}_x$ lattice suppresses superconductivity. This lattice control appears to be through tuning of the interatomic angles in the FeAs layer, with the optimum angle being 110.6° , near the ideal tetrahedral value. The compositional dT_c/dV changes sign around the optimum angle evidencing significant changes in the Fermi surface. It appears difficult to increase the critical temperatures above 56 K in 1111 type iron arsenide materials through tuning lattice effects, although the possibility of higher T_c 's in other structure types remains open.

We acknowledge EPSRC, the Royal Society of Edinburgh and the Leverhulme trust for support.

* Corresponding author: j.p.attfield@ed.ac.uk

Table 1: Synthesis conditions (all samples were synthesised at 10 GPa), refined lattice parameters and volume, T_c 's, mass fractions and superconducting volume fractions for $\text{HoFeAsO}_{1-x}\text{F}_x$ samples.

Sample	t_{synth} (hr)	T_{synth} (°C)	a (Å)	c (Å)	Vol (Å ³)	T_c (K)	Mass frac. (%)	Diamag. frac. (%)
1	2	1150	3.8246(3)	8.254(1)	120.74(3)	29.3	75	70
2	2	1100	3.8272(2)	8.2649(8)	121.06(2)	33.0	74	85
3	1	1150	3.8258(5)	8.264(2)	120.96(4)	33.2	73	76
4	3	1100	3.8282(5)	8.261(2)	121.07(5)	33.7	84	74
5	2	1100	3.8282(2)	8.2654(7)	121.13(2)	35.2	81	57
6	2	1100	3.8297(7)	8.270(2)	121.30(7)	36.2	58	46

Fig. 1 Resistivity and (inset) susceptibility data for an optimum sample of $\text{TbFeAsO}_{0.9}\text{F}_{0.1}$, showing a sharp superconducting transition at $T_c = 51$ K. The sample was prepared at 7 GPa and 1050 °C.

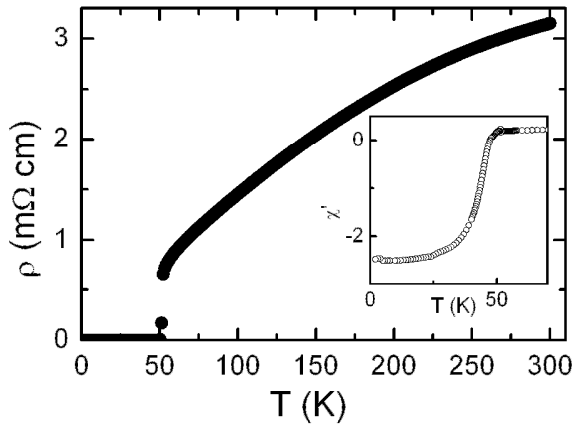


Fig. 2 Fitted x-ray diffraction profile for $\text{HoFeAsO}_{0.9}\text{F}_{0.1}$ (sample 5) at room temperature.

The Bragg markers (from top to bottom) are for the minority phases, Ho_2O_3 and HoAs , and for $\text{HoFeAsO}_{0.9}\text{F}_{0.1}$.

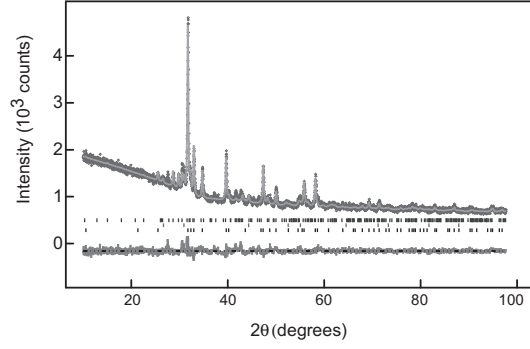


Fig. 3 Superconductivity measurements for $\text{HoFeAsO}_{0.9}\text{F}_{0.1}$; (a) ac magnetic volume susceptibility for the six samples; (b) resistivities for samples 4 and 6.

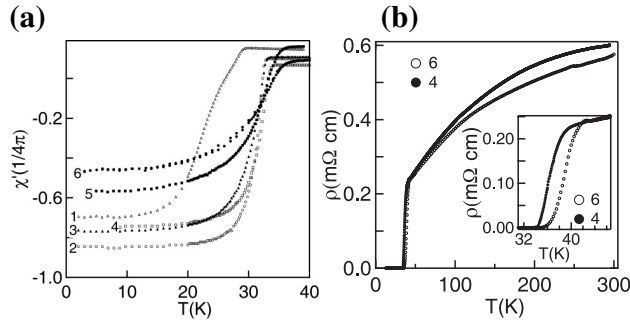


Fig. 4 Variation of Fe-As-Fe angle ϕ (upper panel) and superconducting T_c (lower panel) with unit cell volume for different $R\text{FeAsO}_{1-x}\text{F}_x$ (circles)^{19,22,5,7,12} and $R\text{FeAsO}_{1-\delta}$ (triangles)^{14, 15}. $T_c(\text{max})$ points are shown as filled symbols. The fit of equation $T_c(\text{max}) = T_c(\text{max})_0 \cdot \cos A(\phi - \phi_0)$ with parameters $T_c(\text{max})_0 = 56$ K, $A = 0.03$, and $\phi_0 = 110.6^\circ$ is also shown. dT_c/dV values are derived from the data for sub-optimally doped materials (open symbols) in the $R = \text{La}$,¹⁹ Sm ⁷ and Ho (this paper) systems.

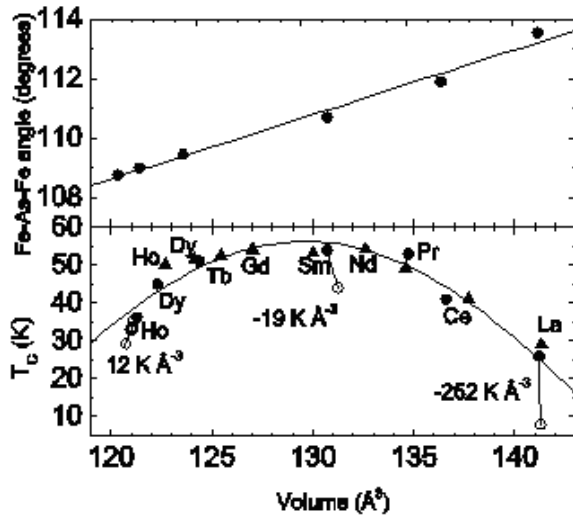
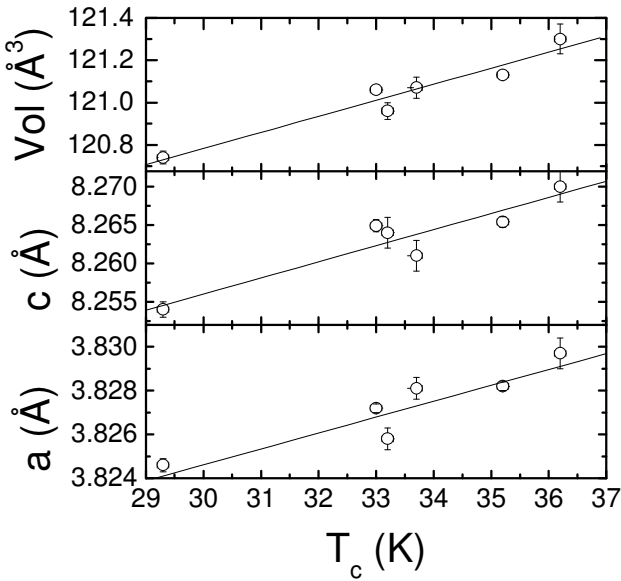


Fig. 5 Variations of T_c with the tetragonal unit cell parameters and volume for the six $\text{HoFeAsO}_{1-x}\text{F}_x$ samples in Table 1.



-
- ¹ P. Quebe, L. J. Terbuchte and W. Jeitschko, *J. Alloys Compounds* **302**, 70 (2000).
- ² J. W. Lynn and P. Dai, *Physica C* **469**, 469 (2009).
- ³ Y. Kamihara, T. Watanabe, M. Hirano and H. Hosono, *J. Am. Chem. Soc.* **130**, 3296 (2008).
- ⁴ H. Takahashi, K. Igawa, K. Arii, Y. Kamihara, M. Hirano, and H. Hosono, *Nature* **453**, 376 (2008).
- ⁵ Z. A. Ren, J. Yang, W. Lu, W. Yi, G. C. Che, X. L. Dong, L. L. Sun, and Z. X. Zhao, *Mater. Res. Innov.* **12**, 105 (2008).
- ⁶ Z. A. Ren, J. Yang, W. Lu, W. Yi, X. L. Shen, Z. C. Li, G. C. Che, X. L. Dong, L. L. Sun, F. Zhou, and Z. X. Zhao, *Europhys. Lett.* **82**, 57002 (2008).
- ⁷ X. H. Chen, T. Wu, G. Wu, R. H. Liu, H. Chen and D. F. Fang, *Nature* **453**, 761 (2008).
- ⁸ Z. A. Ren, W. Lu, J. Yang, W. Yi, X. L. Shen, Z. C. Li, G. C. Che, X. L. Dong, L. L. Sun, F. Zhou, and Z. X. Zhao, *Chin. Phys. Lett.* **25**, 2215 (2008).
- ⁹ R. H. Liu, G. Wu, T. Wu, D. F. Fang, H. Chen, S. Y. Li, K. Liu, Y. L. Xie, X. F. Wang, R. L. Yang, L. Ding, C. He, D. L. Feng, and X. H. Chen, *Phys. Rev. Lett.* **101**, 087001 (2008).
- ¹⁰ P. Cheng, L. Fang, H. X. Yang, X. Zhu, G. Mu, H. Luo, Z. Wang, and H. Wen, *Sci. China. Ser. G* **51**, 719 (2008).
- ¹¹ Samples were synthesised from stoichiometric amounts of RAs, Fe₂O₃, FeF₂ and Fe, using a Walker multianvil module within a 1000 tonne press. The products were dense, black, sintered polycrystalline pellets. Powder X-ray diffraction data were collected on a Bruker AXS D8 diffractometer using Cu K α_1 radiation. Data were recorded at $10 \leq 2\theta \leq 100^\circ$ with a step size of 0.007° for Rietveld analysis. ac magnetic susceptibility was

measured from 3 to 50 K with a field of 0.5 Oe oscillating at 117 Hz using a Quantum Design SQUID magnetometer. Electrical resistivity was measured by a four-probe method between 1.7 and 300 K using a Quantum Design physical property measurement system and an APD cryogenics closed cycle refrigeration unit with an in-house built sample stage.

¹² J.-W. G. Bos, G. B. S. Penny, J. A. Rodgers, D. A. Sokolov, A. D. Huxley and J. P. Attfield, *Chem. Comm.* **31**, 3634 (2008).

¹³ HoFeAsO_{0.9}F_{0.1} has a tetragonal structure (space group P4/nmm; results from fit shown in Fig. 2; goodness of fit $\chi^2 = 1.60$, residuals; $R_{wp} = 3.94\%$, $R_p = 3.02\%$; cell parameters $a = 3.8282(2)$ Å, $c = 8.2654(7)$ Å; atom positions (x,y,z) and isotropic temperature (U) factors; Ho ($\frac{1}{4}, \frac{1}{4}, 0.1454(4)$), $0.044(2)$ Å²; As ($\frac{1}{4}, \frac{1}{4}, 0.6659(5)$), $0.029(2)$ Å²; Fe ($\frac{3}{4}, \frac{1}{4}, \frac{1}{2}$), $0.014(2)$ Å²; O,F ($\frac{3}{4}, \frac{1}{4}, 0$), $0.26(2)$ Å²). The secondary Ho₂O₃ phase is in a high pressure B-type rare earth oxide modification, space group *C2/m*, $a = 13.841(2)$ Å, $b = 3.4984(5)$ Å, $c = 8.608(1)$ Å, $\beta = 100.08(1)^\circ$.

¹⁴ K. Miyazawa, K. Kihou, P. M. Shirage, C. H. Lee, H. Kito, H. Eisaki, and A. Iyo, *J. Phys. Soc. Jpn.* **78**, 034712 (2009).

¹⁵ J. Yang, X. L. Shen, W. Lu, W. Yi, Z. C. Li, Z. A. Ren, G. C. Che, X. L. Dong, L. L. Sun, F. Zhou, and Z. X. Zhao, *New J. Phys.* **11**, 025005 (2009).

¹⁶ J. Zhao, Q. Huang, C. de la Cruz, S. Li, J. W. Lynn, Y. Chen, M. A. Green, G. F. Chen, G. Li, Z. Li, J. L. Luo, N. L. Wang and P. Dai, *Nature Mater.* **7**, 953 (2008).

¹⁷ D. J. Singh and M. -H. Du, *Phys. Rev. Lett.* **100**, 237003 (2008).

¹⁸ The compositional dT_c/dV quantifies the changes in T_c and unit cell volume V due to variations in doping level x at constant (atmospheric) pressure, and is complementary to

the pressure-induced dT_c/dV at constant x . Both derivatives are negative for $\text{LaFeAsO}_{1-x}\text{F}_x$, and we thus predict a positive pressure-induced dT_c/dV (pressure suppression of superconductivity) for $\text{HoFeAsO}_{1-x}\text{F}_x$.

¹⁹ Q. Huang, J. Zhao, J. W. Lynn, G. F. Chen, J. L. Lou, N. L. Wang, and P. Dai, *Phys. Rev. B* **78**, 054529 (2008).

²⁰ S. Lebègue, Z. P. Yin and W. E. Pickett, *New J. Phys.* **11**, 025004 (2009).

²¹ K. A. Yates, K. Morrison, J. A. Rodgers, G. B. S. Penny, J. W. G. Bos, J. P. Attfield, and L. F. Cohen, *New J. Phys.* **11**, 025015 (2009).

²² G. F. Chen, Z. Li, D. Wu, G. Li, W. Z. Hu, J. Dong, P. Zheng, J. L. Luo, and N. L. Wang, *Phys. Rev. Lett.* **100**, 247002 (2008).